Textile Research Journal

Betelnut fibres as an alternative to glass fibres to reinforce thermoset composites: A comparative study

Journal:	*Textile Research Journal*
Manuscript ID:	TRJ-11-0530.R1
Manuscript Type:	Original Manuscript
Keywords:	composites < Materials, strength < Materials, properties < Materials, measurement < Materials, Fabrication < Fabrication

Abstract: For the current work, investigations were carried out using treated betelnut fibre reinforced polyester (T-BFRP) and chopped strand mat glass fibre reinforced polyester (CSM-GFRP) composites. Results revealed that T-BFRP showed competitive performance of about 1.16 %, 17.39 % and 4.92 % for tensile, flexural and compression tests as compared to the latter. Through tribological performance tests, T-BFRP composite showed superiority in wear for the dry and wet tests of about 98 % and 90.8 % while friction coefficient was reduced by about 9.4 % and 80 % respectively. Interface temperature was low by about 17 % for T-BFRP composite subjected to dry test as compared to the latter. SEM analysis revealed that the brittle effects observed on glass fibres during the tribo test enhanced the material removal rate which increased the thermo mechanical effects at the rubbing zone. As such, evidence of adhesive to abrasive wear transition was observed when the CSM-GFRP composite was subjected to the stainless steel counterface. On the contrary, T-BFRP composite formed a thin layer of shield (i.e. back film transfer) on its worn surface during the test which assisted to lower the material removal rate.

Betelnut fibres as an alternative to glass fibres to reinforce thermoset composites: A comparative study

Abstract

For the current work, investigations were carried out using treated betelnut fibre reinforced polyester (T-BFRP) and chopped strand mat glass fibre reinforced polyester (CSM-GFRP) composites. Results revealed that T-BFRP showed competitive performance of about 1.16 %, 17.39 % and 4.92 % for tensile, flexural and compression tests as compared to the latter. Through tribological performance tests, T-BFRP composite showed superiority in wear for the dry and wet tests of about 98 % and 90.8 % while friction coefficient was reduced by about 9.4 % and 80 % respectively. Interface temperature was low by about 17 % for T-BFRP composite subjected to dry test as compared to the latter. SEM analysis revealed that the brittle effects observed on glass fibres during the tribo test enhanced the material removal rate which increased the thermo mechanical effects at the rubbing zone. As such, evidence of adhesive to abrasive wear transition was observed when the CSM-GFRP composite was subjected to the stainless steel counterface. On the contrary, T-BFRP composite formed a thin layer of shield (i.e. back film transfer) on its worn surfaces during the test which assisted to lower the material removal rate.

Keywords

Natural fibre, synthetic fibre, mechanical, wear, friction, polymer-matrix composite

Introduction

Nowadays, fibre reinforced composites are known to be the best substitutes to metals due to their structural properties and availability. Paul et al.[1] and Khan et al.[2] reported that synthetic fibres namely glass and carbon fibres are widely used as composite materials in applications such as: aerospace industries, marine sectors, in the making of sport equipments and automotive components due to their lightweight, responsive strength and rigidity characteristics. Macroscopically, producing synthetic fibres consume high amount of energy [2, 3] which may lead to the contribution of green house effect. Furthermore, Khan et al.[2] reported that synthetic fibres may cause potential health problem to human beings when dealing/processing glass fibres particulates. Interestingly, natural fibres are gaining much attention among researchers namely to explore on the possibility in replacing synthetic fibres. Many researchers agreed on the advantages possessed by natural fibres compared to synthetic fibres. Naming a few, Paul et al.[1] , Joshi et al.[3], Dillon [4], Yousif & El-Tayeb[5] and Nirmal & Yousif [6] revealed in their work that natural fibres are fully biodegradable, low in density, high-specific strength, cheap, aplenty in availability and flexibility in usage.

Over the past decade, many research works[1,2,4,7-9] were carried out to explore the possibility of substituting glass fibres with natural fibres reinforced polymeric composites. Results from the literature reported that glass fibre composites were more superior in mechanical properties compared to natural fibre composites. This is mainly due to the characteristics observed by glass fibres such as their hydrophobic behavior and high fibre specific strength [2, 10]. On the contrary, Paul et al.[1] and Dillon [4] reported that natural fibre can replace glass fibre in applications that do not need high bearing load capacity. In addition, the interest of treating natural fibres using suitable chemical solutions and coupling agents has been proven to boost the mechanical properties of its composites. Sgriccia et al.[10] reported that kenaf fibre treated with

saline coupling agent is equally competitive in mechanical performance when compared to glass fibre composite. Aziz & Ansell [11] reported that 6 % of sodium hydroxide treatment on long kenaf and hemp fibre/polyester composite showed excellent results in mechanical properties compared to glass fibre composite. Nirmal et al.[12] reported that treated betelnut fibre/polyester composites tested under adhesive dry and wet contact conditions had excellent wear performance compared to glass fibre composites. This was due to the high interfacial adhesion strength achieved between the fibre and matrix which prevented fibre pullout during the test. In previous works conducted by Yousif & El-Tayeb [13, 14], the interfacial adhesion of oil palm fibre was highly improved when the fibre was treated with 6 % NaOH due to the disruption of hydrogen bonding in the fibre's network structure. Nevertheless, it directly increased the surface roughness of the fibre. Similar findings were reported by Agrawal et al.[15] where they indicated that a certain amount of oil, lignin and wax covering the outer surfaces of the natural fibre have been removed due to the treatment. As a result of the treatment, it exposes the short length crystallites while depolymerizing the cellulose. On a microscopic point of view, the chemical reaction in Equation 1 shows that the ionization of the hydroxyl group to alkoxide occurs on natural fibres (NF) due to the addition of NaOH.

$$NF - OH + Alkaline\ treatment(NaOH) \Rightarrow NF - O - Na + water(H_2O) \quad \text{(Equation 1)}$$

In summary, Jähn et al.[16] concluded that the alkaline treatment directly influences the extraction of lignin and the polymerization of hemicellulosic compounds and cellulosic fibril which improves surface wettability of natural fibres against the matrix. Besides, the treatment also gave better surface roughness (i.e. removing foreign impurities and entanglements of fine hair) which improved the interlocking characteristics of the fibre and matrix. This phenomenon has been confirmed by Valadez et al.[17] where it was discovered that alkaline treatment has two

effects on the fibre: it increases surface roughness resulting in better mechanical interlocking and ~~it increases the~~ amount of cellulose exposed on the fibre surface, thus increasing the number of possible reaction sites.

Concerning bearing applications, El-Tayeb et al.[18] and Navin et al. [19] reported that glass fibre reinforced polyester (GFRP) composite tested in anti-parallel (AP) orientation with respect to the sliding direction gave high wear resistance compared to parallel (P) and normal (N) orientations. This was due to the formation of a thin layer consisting of broken fibres and fibre pullout from the fibrous region coupled with fragmentation of polyester from the resinous region which assisted in preventing high material removal process during longer sliding distance. El-Tayeb [20] reported that CSM-GFRP composite has better wear resistance compared to short unidirectional sugarcane fibre/polyester composites. However, Yousif & El-Tayeb [21] claimed that oil palm fibre/polyester (OPRP) composite under two body abrasion test showed lower weight loss compared to CSM-GFRP composite due to the high strength of adhesion achieved between oil palm fibre and the matrix. Moreover, the authors stated that a transition from abrasive to adhesive mechanism is possible when fragments of OPRP composite are transferred onto the counterface during the 'detached-attached-detached' process.

For the current work, betelnut fibre~~s~~ is proposed as a potential commercial substitute to CSM glass fibre for reinforcement~~s~~ in polymeric composites due to variety of reasons. For an instance, betelnut fibre has low fibre density (i.e. fully renewable and recyclable [6], lower abrasiveness to machines, ~~having no health risk~~non hazardous to health [2] and ~~being~~ fully biodegradable [6, 12] compared to glass fibres. Besides that, Nirmal & Yousif [6], Nirmal, Singh, Hashim, Lau & Jamil [22] and Nirmal [23]have reported in their work that betelnut fruits are highly abundant in Malaysia. Looking at the chemical composition in betelnut fibre husks (refer Table

1); the fibres are composed of varying proportions of cellulose, lignin, pectin and protopectin which makes them a good substitute for reinforcement purposes. For an instance, Jacob et al.[24] and Khalil et al.[25] reported in their findings that the content of cellulose in certain natural fibres makes them highly hydrophilic (attracts water) which leads to more water uptake by the cell walls of the fibres surfaces and thus weakening its fibre properties; i.e. tensile strength. On the other hand, betelnut fibres have certain percentage of lignin on its outer fibre surfaces making it hydrophobic, thus, preventing large amount of water absorption into the fibre core.[10] Additionally, the decaying of betelnut fibre husks when composted to the soil will result in the production of nitrogen, potassium pentoxide and potassium oxide[26]. Ramachandra et al.[26] indicated in their work that these chemical substances are important to the soil as they acts as fertilizers, thus increasing the soil fertility. The above findings are summarized in Table 2 highlighting the main difference between betelnut and CSM glass fibres. From the table, it is obvious that betelnut fibres are more favorable as compared to CSM glass fibres.

In regard to the above considerations, the authors found an interest to use betelnut vs. glass fibres as potential reinforcing elements in polymeric composites aiming to explore on the mechanical and tribological performance of these composites. Tensile, flexural, compression and hardness properties of the developed composites have been investigated based on ASTM [27-29] standards. For the tribological tests, a developed Block on Disc (BOD) machine has been used to simulate the wear and friction performance of the T-BFRP and CSM-GFRP composites subject to dry and wet contact conditions. The adhesive sliding of the composite was conducted on a smooth stainless steel counterface at sliding velocity of 2.8 m/s at applied loads of 30 N and 200 N for dry and wet contact conditions. Based on the results obtained, a comparative study was

performed on the potential substitution of CSM-GFRP with T-BFRP composite in relevant applications.

Materials preparation

Preparation of fibres

Raw betelnut fruits (c.f. Fig. 1a) are found abundant, in particular state of Kedah, Malaysia. The betelnuts have to be crushed first in order to remove the seeds. The crushed betelnuts were then rinsed and soaked in water for two days to ease of fibre extraction process. While still wet, the outer layers of the betelnut fruit were removed followed by extraction of the fine fibres (c.f. Fig. 1b) using a fibre-extractor-machine-with-bubbling-wash-effect (FEM-BWE) which was previously designed and fabricated by Nirmal [31]. Then, the extracted fibres (c.f. Fig. 1c) were treated in water containing 6 % Sodium Hydroxide (NaOH) solution for half an hour at room temperature (28 ± 2 ^{o}C). This was done to remove foreign substances on the fibre and to enhance the adhesion characteristics between the fibre and the matrix. The fibres were then taken out from the solution and rinsed with fresh water to remove the NaOH solution. Finally, the cleaned and treated fibres were arranged in a randomly distributed manner, pressed evenly into uniform mats (c.f. Fig. 1d) and left to dry at room temperature (28 ± 2 ^{o}C). In order to ensure effective drying of the betelnut fibres, all treated betelnut fibre mats were dried in an oven for 5 hours at 45 ºC. Figs. 2a & b show significant differences of the betelnut fibre before and after the treatment. A very rough surface can be seen on the treated one, Fig. 2b, as compared to the untreated, Fig. 2a. This is due to the significant effects of the cleaned tiny hairy spots which protrude out from the surface of an individual betelnut fibre termed *trichomes.* They are defined as ‘epidermal hairs found on nearly all plants taking almost various shapes and forms’ [31].

Therefore, the present of *trichomes* by nature on the outer surface of the betelnut fibre may help improve interfacial adhesion strength of the fibre (i.e. high fibre surface roughness) in the mat against the matrix by minimizing fibre pullout and debonding during sliding. For chopped strand mat glass fibres; Fig. 2c, it was obtained from Poly Glass Fibre Manufacturing Sdn. Bhd., Malaysia.

For the purpose of preparing the fibre mats (i.e. betelnut and glass fibres), all fibre mats were cut into the dimensions of the composite fabrication mold. The corresponding SEM images showing the randomly distributed betelnut and CSM glass fibre in mat form are ~~is~~ presented in Fig. 3. Table 3 summarizes basic properties of the betelnut and CSM glass fibre mats.

Preparation of composite

Unsaturated polyester (Butanox M-60) mixed with 1.5 % of Methyl Ethyl Ketone Peroxide (MEKP) as a catalyst was selected as a resin for the current work. Information of the resin and hardener is listed in Table 4 respectively [32].

The resin and hardener were uniformly mixed using an electrical stirrer and poured into a closed mold with a size of 100 mm x 100 mm x 10 mm. The inner surfaces of the mold ~~had been~~were sprayed with a thin layer of silicon as a release agent. Hand lay-up technique was used, by which the first layer of the composite material was obtained by pouring the unsaturated polyester (mixed with 1.5 wt% hardener) into the mold. Subsequently, a sheet of betelnut fibre mat was placed on the first layer of polyester. A steel roller was used to even out the fibre mat and to release air bubbles from the mixture. This procedure was repeated until a maximum thickness of 10 mm was achieved (resulting with 13 layers of fibre mats and 14 layers of polyester resin). Then, a thin steel plate of same size with the mold was placed on top of the

mold's opening pressing the composite. A pressure of about 5 kPa was applied on the steel plate to ensure that the trapped air bubbles in the composite were completely forced out. With the pressure still being applied on the mold, the composite block was left to cure for 24 hours at room temperature (28 ± 2 °C). For thoroughness in curing, the hardened composite was removed from the mold and post-cured in an oven at 80 °C for one hour. Similarly, the CSM-GFRP composite block was fabricated using the steps explained above.

For the purpose of conducting the mechanical tests, the cured composite blocks (i.e. T-BFRP and CSM-GFRP composites) wereas machined into the required sizes of test samples, i.e. tensile, flexural and compression samples. Fig. 4 shows the dimensions of the prepared samples according to ASTM standards [27-29].

For tribological tests, the test specimens with dimensions of 10 mm x 10 mm x 20 mm had beenwere prepared from the cured composite block using a Black and Decker jigsaw (Model: CD301-B1). SEM images of the virgin cross section of T-BFRP and CSM-GFRP composite test specimen is displayed in Fig. 5a & b. From the figures, the approximate thickness of the polyester layer is about 130 ± 15 µm. A schematic view of the tribological test specimen showing its orientation of fibre mats with respect to the sliding direction is displayed in Fig. 5c.

Experimental procedure

Mechanical test

Tensile, flexural and compression tests have beenwere conducted using a WP300 PC Aided Universal Material Test machine at room temperature (28 ± 2 °C). Moreover, a hardness tester (Model: TH210 ShoreD durometer) has beenwas also used to determine the ShoreD hardness of the composites. The hardness was measured perpendicular to the fibre orientation of the

polyester composite (perpendicular to the thickness of 10 mm for the compression test specimen, c.f. Fig. 4c).

Tribological test

A Block-On-Disc (BOD) machine subjected to dry and wet contact conditions was used for the current work. Water (hardness: 120 - 130 mg/liter) was supplied to the counterface by a pump at a flow rate of 0.4 l/min. Water flowing off the counterface was ~~collected~~ contained by a container, with a filter being placed along the flow of water. It was cleaned from the generated wear debris after each test. An Accutec B6N-50 load cell was incorporated in the BOD load lever in order to measure the frictional forces between the specimen and the counterface. The load cell was connected to a digital weight indicator (Model: Dibal VD-310) in order to capture the frictional forces during the test. For measuring the interface temperature (i.e. temperature between test specimen and counterface), a thermocouple (Model: Center 306) was adopted where the thermocouple probe was placed at the test specimen contacting area with the counterface. Accordingly, temperature measurements were recorded for every one minute of time interval for all dry and wet testing conditions.

In a similar work done by Tong et al.[33] subject to dry contact conditions, a higher PV limit of polyester of 1.61 MPa·m/s was achieved. Accordingly, for the current work, the PV limit achieved was between 0.14 - 0.84 MPa·m/s (equivalent 30 N applied load at 2.8 m/s sliding velocity) for the dry conditions. It is to be noted here that 30 N of applied normal load was chosen for comparing the wear performance of the developed composites since at this load, there was obvious differences in the values of Ws. At lower range of applied loads (i.e. 5 – 10 N), Ws was not that significant for comparison. At higher loads (>30 N), the composite failed due to the

high thermo mechanical loading incurred by the test specimens during the adhesive dry sliding test. On the other hand, under wet contact conditions, the weight loss could not be determined at low applied load (30 N) due to the low weight loss (less than 0.1 mg). Therefore, the wet tests were conducted at higher applied loads of 200 N at 2.8 m/s sliding velocity. The tests were performed at different sliding distances (0 - 6.72 km). The critical load was 200 N for the wet test due to the limitation of the load cell as confirmed by the supplier of the load cell, i.e. maximum loading capacity of the load cell ≤ 20 kg.

Before each test, the composite test specimen was loaded into the specimen holder and abrasive paper of grade 800 was placed between the counterface and the test specimen. With a normal load of 20 N applied, the counterface was turned manually to achieve sufficient intimate contact. This procedure was repeated on the same test specimen but with a different abrasive paper of ~~with~~ grade 1000. ~~abrasive paper instead~~. This was to minimize mechanical interlocking of the specimen against the counterface during testing. Upon completion, the test specimen was taken out, cleaned with a wet cloth, dried and weighed using a weighing scale (Model: Setra weight balance ± 0.1 mg) before the experiment.

Concerning the stainless steel counterface, it was polished with abrasive papers starting with grade 200, 500, 1000 followed by 2000. After polishing, the counterface was cleaned with liquid acetone by means of a clean cloth. To avoid conflict in friction readings generated during the test which might be influenced from any thin layer of acetone remaining behind during the counterface cleaning process, the whole counterface was wiped with a wet cloth and dried at room temperature (28 ± 2 °C) before each test. This procedure was repeated for all dry and wet tests. For the wet tests, all specimens were dried in an oven at temperature of 40 ºC for 24 hours.

The specific wear rate was computed using Equation 2. The weight losses of the specimen ~~have been~~ were determined using a Setra weight balance (± 0.1 mg).

$$W_S = \frac{\Delta V}{F_N . D} \quad \text{(Equation 2)}$$

where; W_s = Specific wear rate [mm^3/N·m]

ΔV = Volume difference [mm^3]

F_N = Normal applied load [N]

D = Sliding distance [m]

Results and discussions

As a result of repeating the mechanical and tribological experiments for three times, the standard deviation is computed which is presented in Fig. 6.

It is to be highlighted here that, due to the nature of the betelnut fibre husks being fine and short, it was impossible for uni-directional or bi-directional layout. Thus, randomly distributed fibres were preferred during composite fabrication. For comparing purposes and on the prospect of potential substitution in mechanical and tribological applications of polymeric composites, chopped strand mat (CSM) glass fibre was used as comparison since it possesses close or similar characteristics to betelnut fibres (i.e. randomly distributed).

Mechanical performance of T-BFRP vs. CSM-GFRP composites

Mechanical performance of the T-BFRP and CSM-GFRP composites are presented in Fig. 7. A visual examination on Fig. 7a reveals different trends of mechanical properties for the two types

of composites, i.e., T-BFRP vs. CSM-GFRP. It can be seen that the T-BFRP composite exhibits competitive performance in tensile, flexural and compression strength compared to the CSM-GFRP composite. From the figure, the T-BFRP composite showed up to 1.16 %, 17.39 % and 4.92 % in variation for tensile, flexural and compression tests compared to the latter.

With fibre to resin ratio of about 48 %vol used during composite fabrication for both betelnut and CSM glass fibres, the T-BFRP composite has hardness of about 8.54 % higher compared to CSM-GFRP; Fig. 7b. Thus, as suggested by Tsukada et al.[34] and Hariharan et al. [35], T-BFRP composite can be made applicable to applications where hardness is of an important factor such as in the making of partition boards, doors, window panels and ceilings.

Though betelnut fibres' mechanical properties (i.e. tensile, flexural & compression) are lower than those of glass fibres, their specific properties, especially fibre stiffness, is ~~are~~ comparable to the stated values of glass fibres. Fig. 8 shows a typical average load-displacement diagram for the glass and treated betelnut fibre through single fibre pullout test (SFPT). The figure indicates that the betelnut fibre exhibits ductile like behavior during the test where the maximum pullout force was about 16 N at fibre elongation of about 4 mm. However, glass fibre exhibits a maximum pullout force of about 17 N at a shorter fibre elongation of about 1.5 mm, (i.e. brittle behavior).

Tribological performance of T-BFRP vs. CSM-GFRP composites

The wear and frictional performance of the T-BFRP and CSM-GFRP composites at dry and wet contact conditions are presented in Figs. 9a & b. T-BFRP composite showed superiority in wear of about 98 % for dry and 90.8 % for wet tests while the friction was low by about 9.4 % and 80 % for the dry and wet tests compared to the latter. These significant improvements in wear and

friction property propose the T-BFRP composite to be a potential candidate to substitute the latter concerning applications related to tribology. Further analysis on the worn surfaces of the composites will be discussed below with the assistance of SEM images.

Temperature performance of T-BFRP vs. CSM-GFRP composites

The temperature performance for T-BFRP and CSM-GFRP composites at dry and wet contact conditions are presented in Fig. 10. Fig. 10a shows the temperature profiles of the two different composites at different sliding distances. The measurements were taken at every one minute of time interval for a total sliding distance of 6.72 km throughout the dry and wet tribological tests.

From Fig. 10a, it can be seen that there is a gradual increment between the interfaces temperature (< 4.5 km) for both composites subjected to dry contact condition. This is namely due to the effect of thermo mechanical loading evidenced during adhesive dry sliding. At longer sliding distance (> 4.5 km), temperature rise was more significant due to the fact that there was severe plastic deformation by the composites. Hence, the resinous regions were easily deformed thereby lowering the adhesion of fibres/matrix which enhanced the material removal process. Further examination of the composite worn surfaces will be discussed as below with the assistance of SEM images. When the composites were subjected to wet contact conditions, the effect of thermo mechanical loading was completely eliminated when water was supplied to the interfaces (i.e. test specimen and counterface). Thus, interface temperature of the T-BFRP and CSM-GFRP composite test specimens was constant throughout the test which is confirmed by the temperature profiles in Fig. 10a. To see the effect of different fibre reinforcements in

polyester composites on average interface temperatures, Fig. 10b is presented. From the figure, reinforcing polyester with betelnut fibres have lowered the interface temperature by about 17% compared to glass fibres under dry adhesive test. Interface temperature for CSM-GFRP composite was high due to the brittle effects of glass fibres which could influence the transition of wear mechanism from adhesive to abrasive between the interacting zones (i.e. test specimen and counterface). In the case of wet contact condition, supplied water at the interfaces kept the interacting surfaces clean from generated wear debris while maintaining the contact temperature constant throughout the test.

To further clarify the results, Fig. 11 is presented where it explains the possible wear mechanism that took place during the adhesive wear test subjected to dry and wet contact conditions for the T-BFRP and CSM-GFRP composites. From Fig. 11a, when the composite test specimen (soft) is in contact with the stainless steel counterface (hard), three contact mechanism may had took place. They are known as ‘cold welding’ and ‘rupture’ due to the uneven surface of the test specimen. Besides that, fine wear particles which can’t be detected by the naked eyes may have also been present between the interfaces. When the sliding starts, rupture of the uneven surface from the test specimen takes place causing a third body between the interfaces. This third body (from the resinous or fibrous region) with the trapped wear particles might have been in circular or linear motion between the interfaces during the adhesive dry sliding causing film transfer onto the counterface. Therefore, possible wear mechanism on the top surface of the film transfer could be ‘galling’ (due to circular motion of wear debris between the interfaces) or ‘scoring’ (due to linear motion of wear debris between the interfaces). This can cause high resistance of relative motion during the adhesive dry test and thus contributing to a much higher interfaces temperature.

On the contrary, Fig. 11b illustrates a different sliding mechanism for the wet test during start up. From the figure, the gap formed between the composite test specimen and the counterface due to the formation of 'cold welding' and trapped wear particles is now filled with water. It is also to be highlighted here that water was introduced to the counterface before the adhesive wet test was carried out. Hence, during the test, deformation of 'cold welding' and rupture of the uneven joints of the composite test specimen were~~was~~ instantly washed away from the interfaces with the help of flowing clean water. This eliminates the presence of third body (from the resinous or fibrous region) and the formation of film transfer at the interface. Thus, the ease of relative motion due to the presence of water contributes to a drastic drop in static to kinetic friction coefficient. Besides, thermo-mechanical loading is also eliminated since water had also played a role to keep the counterface temperature constant throughout the test.

Morphology of the worn surfaces through SEM analysis

Surface morphology of the samples was analyzed through SEM (model: EVO 50 ZEISS-7636). Before taking the SEM images, the samples were coated with a thin layer of gold using ion sputtering (model: JEOL, JFC-1600). All observing conditions were performed at room temperature of 28 ± 5 ^{o}C and at humidity level of 80 ± 10 %.

The worn surfaces for the different composites subjected to dry contact condition at 1000X magnification is presented in Fig. 12. Different wear features are evidenced on the worn surfaces subjected to different fibre reinforcements in polyester composites. An obvious sign of plastic deformation can be observed at the resinous regions for the T-BFRP composite associated with sign of soften polyester, Fig. 12a. This is due to the high intimate contact of the test specimen and counterface yield the polyester to melt with the influence of severe thermo

mechanical loading at longer sliding distances, 6.72 km. In regard to this, part of the fibres received poor support from the polyester matrix which contributed to the high material removal rate, i.e. from the fibrous regions. This is confirmed with the sign of fine debris evidenced on the worn surface. On the other hand, there were signs of embedded fibres in the matrix on the worn surface, Fig. 12a. This could be due to the effects of *trichomes* on the betelnut fibre surfaces which assisted to lock the fibres firmly in the matrix preventing complete fibre pullout.

On the contrary, the wear damage was much significant when CSM-GFRP composite was subjected to the counterface, Fig. 12b. It can be seen that the glass fibre wasere deformed at longer sliding distance, 6.72 km. Besides that, there was also sign of fractured and deformed polyester at the resinous regions. This further caused damage onto the glass fibre, i.e. the fibre was easily broken apart due to the excessive sliding shear force by the worn polyester debris. Arguably, the combined brittle nature of worn polyester debris and glass fibres led to the formation of fine/coarse abrasive wear particles as evidenced in Fig. 12b. This further reduced the wear performance of the composite namely when these particles interacted at the contacting zones by enhancing the material removal rate by a factor of 99e-8 $mm^3/m{\cdot}N$ compared to the T-BFRP composite (c.f. Fig. 10a). Moreover, loose abrasive particles and polyester debris at the rubbing zone assisted to increase the friction coefficient and interfaces temperature which is confirmed by Fig. 9b and Fig. 10.

Due to the fact that T-BFRP composite revealed less damage than the CSM-GFRP composite, possible suggestion of the proposed T-BFRP composite can be in non-structural applications [1, 4] since many attempts have been made to use natural fibre composites in place of glass fibre composites. Addition to this, Dahlke et al.[36], Quig et al. [37], Fukuhara [38] and Leao et al.[39] reported that a good number of automotive components previously made with glass fibre

composites are now being manufactured using environmentally friendly composites. Moreover, Eberle & Franze [40] further claimed that automotive giants such as Daimler Chrysler and Mercedes Benz are continuously producing low weight vehicles over the recent years using huge amount of renewable fibres in composite fabrication since for every 1 kg of weight reduction of an automobile vehicle, as much as 5.95 to 8.4 liters of petrol can be saved. Secondly, as suggested by Bhushan [41] and Cirino et al.[42], the proposed T-BFRP composite can be used as bearing and sliding materials subjected to tribological loading conditions due to their low friction conditions (i.e. wet conditions), high wear resistance and easy process ability properties.

Though T-BFRP composite offer several benefits as compared to CSM-GFRP composite, several major technical considerations must be addressed before the engineering, scientific and commercial communities gain the confidence to enable wide-scale acceptance, particularly in exterior parts where a Class A surface finish is required. To name but a few, these challenges include in depth investigation on the homogenization of the fibres' properties and a full understanding of the degree of polymerization and crystallization, adhesion between the fibre and matrix, moisture repellence, and flame retardant properties.

Conclusions

Based on the results obtained, the following conclusions are drawn:

1. Betelnut fibres have commercial benefits. This may be attributed to the surface roughness of the *trichomes* which enhance the interlocking of the betelnut fibre in the matrix and the peculiar property of the betelnut fibrous region itself.
2. In mechanical properties, T-BFRP composite was found to have equivalent property in tensile and compression strengths while flexural strength was lower by about 15% compared to CSM-GFRP composite. Hardness test for the T-BFRP composite was 10 % superior compared to CSM-GFRP composite.
3. In tribological properties, specific wear rate for T-BFRP composite was low by about 98% and 90.8% in both dry and wet tests compared to CSM-GFRP composite. Meanwhile the friction coefficient for T-BFRP composite was reduced by about 9.4 % and 80 % for the dry and wet tests as compared to the latter. Interfaces temperature of the T-BFRP composite was 17% lower for the dry test as compared to the CSM-GFRP composite. Under wet contact conditions, both composites did not show any significant effects of interfaces temperature.

Acknowledgements

The authors would like to thank Chan Wai Ti for his kind support and help contributed towards the implementation of this research.

References

1. Paul W, Jan I and Ignaas V. Natural fibres: can they replace glass in fibre reinforced plastics? . *Composites Science and Technology*. 2003; 63: 1259-64.
2. Khan RA, Khan MA, Zaman HU, et al. Comparative studies of mechanical and interfacial properties between jute and E-glass fibre reinforced polypropylene composites. *Journal of Reinforced Plastics and Composites*. 2010; 29: 1078-88.
3. Joshi SV, Drzal LT, Mohanty AK and Arora S. Are natural fibre composites environmentally superior to glass fibre reinforced composites? *Composites Part A: Applied Science and Manufacturing*. 2004; 35: 371-6.
4. Dillon JH. Current Problems and Future Trends in Synthetic Fibres. *Textile Research Journal*. 1953; 23: 298-312.
5. Yousif BF and El-Tayeb NSM. Adhesive wear performance of T-OPRP and UT-OPRP composites. *Tribology Letters*. 2008; 32: 199-208.
6. Nirmal SG and Yousif BF. Wear and frictional performance of betelnut fibre-reinforced polyester composite. *Proceedings of the Institution of Mechanical Engineers, Part J: Journal of Engineering Tribology*. 2009; 223: 183-94.
7. Rodriguez E, Petricci R, Puglia D, Kenny JM and Vazquez A. Characterization of composites based on natural and glass fibres obtained by vacuum infusion. *Journal of Composite Materials*. 2005; 39: 265-82.
8. Shubhra QTH, Alam AKMM and Beg MDH. Mechanical and degradation characteristics of natural silk fibre reinforced gelatin composites. *Materials Letters*. 2011; 65: 333-6.
9. Meiwu S, Hong X and Weidong Y. The Fine Structure of the Kapok Fibre. *Textile Research Journal*. 2010; 80: 159-65.
10. Sgriccia N, Hawley MC and Misra M. Characterization of natural fibre surfaces and natural fibre composites. *Composite: Part A*. 2008; 39: 1632-7.
11. Aziz SH and Ansell MP. The effect of alkalization and fibre alignment on the mechanical and thermal properties of kenaf and hemp bast fibre composites: Part 1 - polyester resin matrix. *Composites Science and Technology*. 2004; 64: 1219-30.

12. Nirmal U, Yousif BF, Rilling D and Brevern PV. Effect of betelnut fibres treatment and contact conditions on adhesive wear and frictional performance of polyester composites. *Wear*. 2010; 268: 1354-70.
13. Yousif BF and El-Tayeb NSM. High-stress three-body abrasive wear of treated and untreated oil palm fibre-reinforced polyester composites. *Proceedings of the Institution of Mechanical Engineers, Part J: Journal of Engineering Tribology*. 2008; 222: 637-46.
14. Yousif BF and El-Tayeb NSM. Wet adhesive wear characteristics of untreated oil palm fibre-reinforced polyester and treated oil palm fibre-reinforced polyester composites using the pin-on-disc and block-on-ring techniques. *Proceedings of the Institution of Mechanical Engineers, Part J: Journal of Engineering Tribology*. 2010; 224: 123-31.
15. Agrawal R, Saxena NS, Sharma KB, Thomas S and Sreekala MS. Activation energy and crystallization kinetics of untreated and treated oil palm fibre reinforced phenol formaldehyde composites. *Materials Science and Engineering A*. 2000; 277: 77-82.
16. Jähn A, Schröder MW, Füting M, Schenzel K and Diepenbrock W. Characterization of alkali treated flax fibres by means of FT Raman spectroscopy and environmental scanning electron microscopy. *Spectrochimica Acta Part A: Molecular and Biomolecular Spectroscopy*. 2002; 58: 2271-9.
17. Valadez GA, Cervantes UJM, Olayo R and Herrera FPJ. Effect of fibre surface treatment on the fibre-matrix bond strength of natural fibre reinforced composites. *Composites Part B: Engineering*. 1999; 30: 309-20.
18. El-Tayeb NSM, Yousif BF and Yap TC. Tribological studies of polyester reinforced with CSM 450-R-glass fibre sliding against smooth stainless steel counterface. *Wear*. 2006; 261: 443-52.
19. Navin C, Ajay N and Somit N. Three-body abrasive wear of short glass fibre polyester composite. *Wear*. 2000; 242: 38-46.
20. El-Tayeb NSM. Two-body abrasive behaviour of untreated SC and R-G fibres polyester composites. *Wear*. 2009; 266: 220-32.

21. Yousif BF and El-Tayeb NSM. Mechanical and Wear Properties of Oil palm and glass fibres reinforced polyester composites. *International journal of precision engineering*. 2009; 1 213-22.
22. Nirmal, U., Singh, N., Hashim, J., Lau, S.T.W. and Jamil, N. On the effect of different polymer matrix and fibre treatment on single fibre pullout test using betelnut fibres, *Materials & Design*, 2011; vol. 32, pp. 2717-2726.
23. Nirmal, U. "Betelnut fibres as bio-reinforcements in polyester composites for mechanical and tribological applications," *Faculty of Engineering and Technology*, Multimedia University, Malacca, 2011, p. 142.
24. Jacob M, Varughese KT and Thomas S. Water sorption studies of hybrid biofibre-reinforced natural rubber biocomposites. *Biomacromolecules*. 2005; 6: 2969–679.
25. Khalil HPSA, Ismail H, Rozman HD and Ahamad MN. The effect of acetylation on interfacial shear strength between plant fibres and various matrices. *Eur Polym J*. 2001; 37: 1037-45.
26. Ramachandra TV, Kamakshi G and Shruthi BV. Bioresource status in Karnataka. *Renewable and Sustainable Energy Reviews*. 2004; 8: 1–47.
27. D790 AS. Standard Test Method Flexural Properties of Unreinforced and Reinforced Plastics and Electrical Insulating Materials. West Conshohocken, PA: ASTM International, 2010.
28. D695 AS. Standard Test Method for Compressive Properties of Rigid Plastics. West Conshohocken, PA: ASTM International, 2010.
29. D638 AS. Standard Test Method for Tensile Properties of Plastics. West Conshohocken, PA: ASTM International, 2010.
30. Foulk J, Akin D and Dodd R. New low cost flax fibres for composites. Detroit: SAE World Congress, 2000.
31. Nirmal SG. An Investigation of Wear and Frictional Performance of Betelnut Fibre Reinforced Polyester Composite Under Dry Contact Condition. *Faculty of Engineering and Technology*. Malacca: Multimedia University, 2008, p. 100.

32. Akzo Nobel Polymer Chemicals. SAFETY DATA SHEET According to Regulation (EC) No. 1907/2006 BUTANOX M-60 http://www.yucelkompozit.com.tr/images2/File/MSDS_PRD_BUTANOX%20M-60%20(English).pdf (2006, accessed 12 December 2011).
33. Tong J, Ma Y, Chen D, Sun J and Ren L. Effects of vascular fibre content on abrasive wear of bamboo. *Wear*. 2005; 259: 78-83.
34. Tsukada M, Md. Majibur Rahman K, Tanaka T and Morikawa H. Thermal characteristics and physical properties of silk fabrics grafted with phosphorous flame retardant agents. *Textile Research Journal*. 2011; 81: 1541-8.
35. Hariharan ABA and Khalil HPSA. Lignocellulose-based Hybrid Bilayer Laminate Composite: Part I - Studies on Tensile and Impact Behavior of Oil Palm Fibre-Glass Fibre-reinforced Epoxy Resin. *Journal of Composite Materials*. 2005; 39: 663-84.
36. Dahlke B, Larbig H, Scherzer HD and Poltrock R. Natural Fibre Reinforced Foams Based on Renewable Resources for Automotive Interior Applications. *Journal of Cellular Plastics*. 1998; 34: 361-79.
37. Quig JB and Dennison RW. The Complementary Nature of Fibres from Natural and from Synthetic Polymers. *Textile Research Journal*. 1954; 24: 361-73.
38. Fukuhara M. Innovation in Polyester Fibres: From Silk-Like to New Polyester. *Textile Research Journal*. 1993; 63: 387-91.
39. Leao A, Rowell R and Tavares N. Applications of natural fibres in automotive industry in Brazil-thermoforming process. Cairo, Egypt: Plenum press, 1997, p. 755–60.
40. Eberle R and Franze H. Modeling the use phase of passenger cars in LCI. Graz Austria: SAE Total Life-cycle Conference, 1998.
41. Bhushan B. *Principles and applications of tribology*. New York: Wiley, 1999.
42. Cirino M, Friedrich K and Pipes RB. Evaluation of polymer composites for sliding and abrasive wear applications. *Composites*. 1988; 19: 383-92.

Figure legend

Fig. 1: Steps of betelnut fibre preparation

Fig. 2: Micrographs of glass fibres, untreated and treated betelnut fibres

Fig. 3: SEM images showing randomly distributed betelnut and CSM glass fibre in mat form

Fig. 4: Schematic illustration of different test specimens for conducting the mechanical test

Fig. 5: SEM of the virgin test specimens and corresponding schematic illustration of the specimen showing fibre orientation and sliding direction

Fig. 6: Corresponding standard deviation for the different types of composites

Fig. 7: Mechanical performance of T-BFRP and CSM-GFRP composites

Fig. 8: SFPT for glass and treated betelnut fibre

Fig. 9: Tribological performance of T-BFRP and CSM-GFRP composites

Fig. 10: Temperature performance of the T-BFRP and CSM-GFRP composites at dry and wet conditions

Fig: 11: Adhesive sliding mechanism for dry and wet contact conditions wet conditions

Fig. 12: SEM images of the T-BFRP and CSM-GFRP composites at dry contact condition subjected to an applied load of 30 N, 6.72 km sliding distance and 2.8 m/s of counterface sliding velocity

List of tables

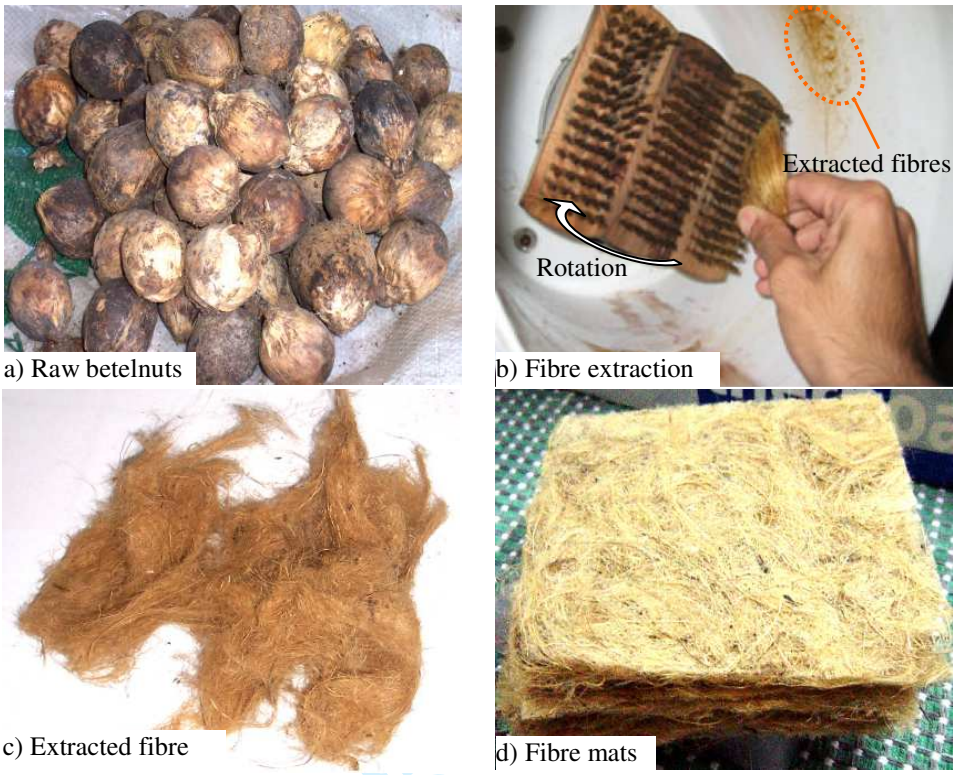

Fig. 1: Steps of betelnut fiber preparation

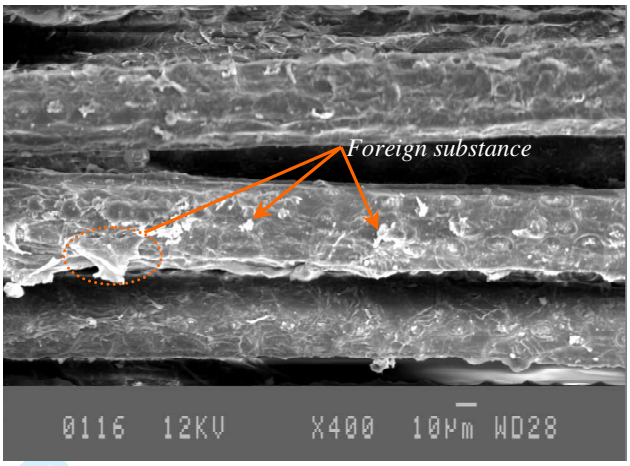

a) Untreated betelnut fibers

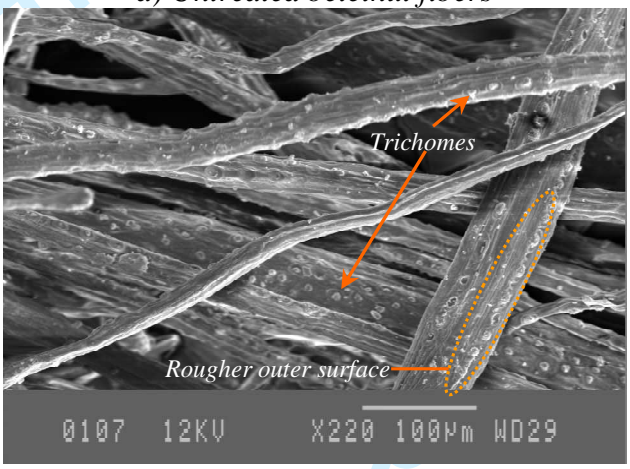

b) Treated betelnut fibers

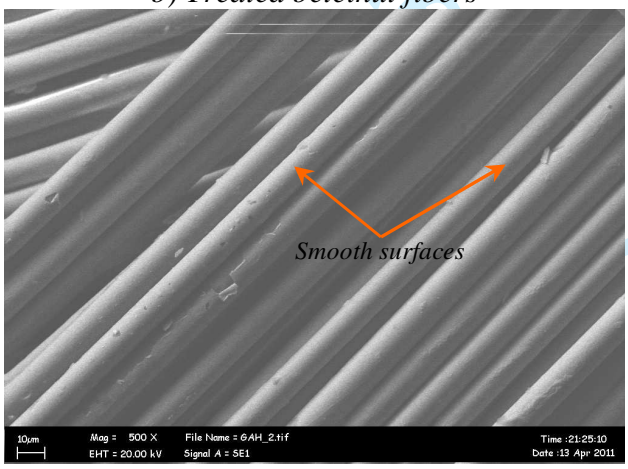

c) Glass fibres

Fig. 2: Micrographs of glass fibres, untreated and treated betelnut fibers

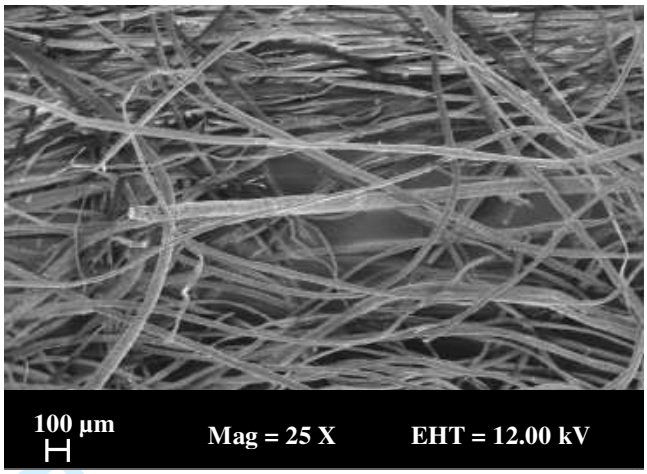

a) Betelnut fiber mat

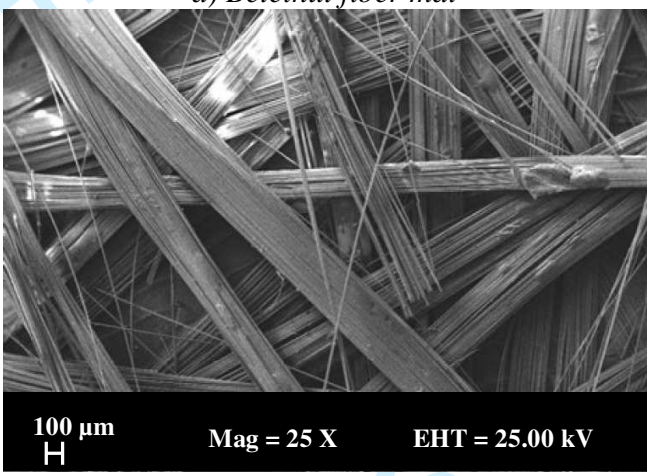

b) CSM glass fiber mat

Fig. 3: SEM images showing randomly distributed betelnut and CSM glass fiber in mat form

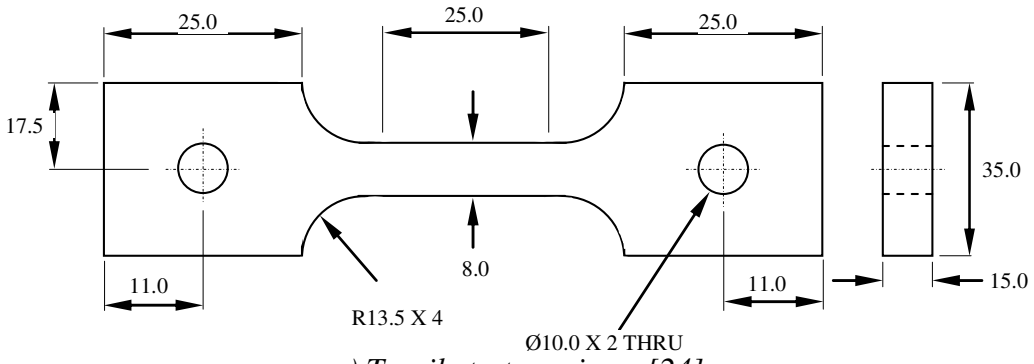

a) Tensile test specimen [24]

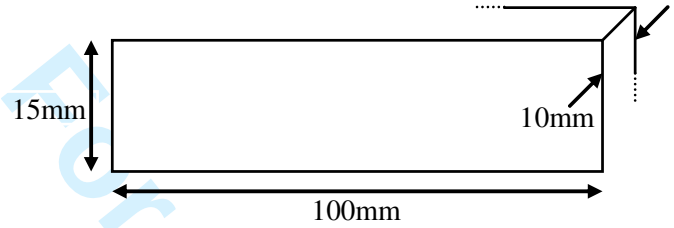

b) Flexural test specimen [25]

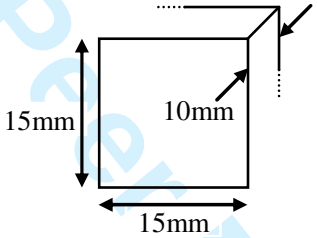

c) Compression and hardness test specimen [26]

Fig. 4: Schematic illustration of different test specimens for conducting the mechanical test

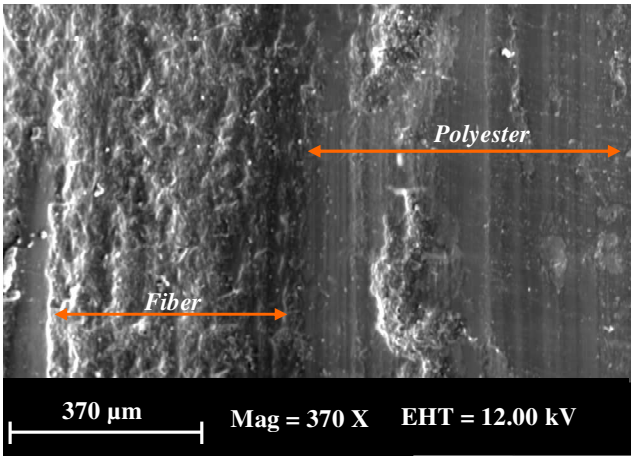

a) Virgin surface of the T-BFRP composite test specimen

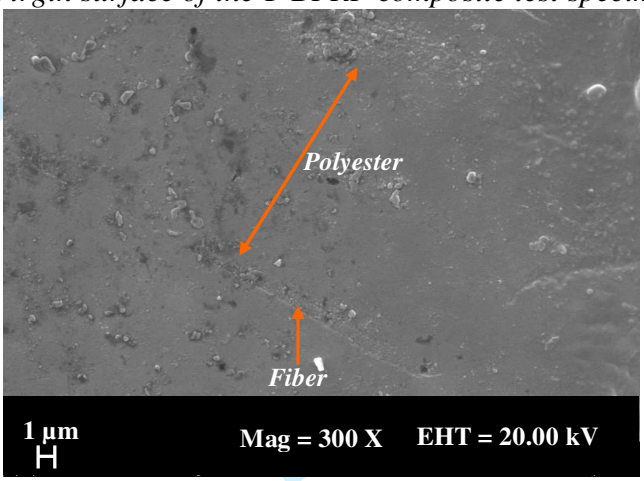

b) Virgin surface of the CSM-GFRP composite test specimen

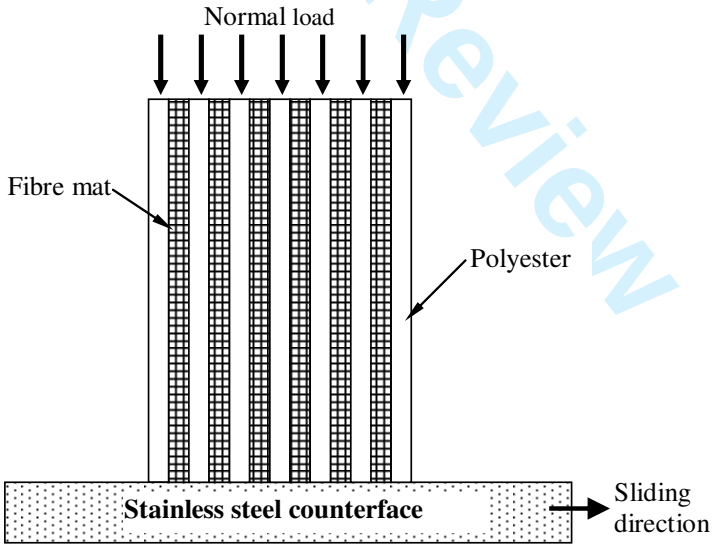

c) Schematic illustration of T-BFRP composite showing fiber mats orientation with respect to the sliding direction

Fig. 5: SEM of the virgin test specimens and corresponding schematic illustration of the specimen showing fibre orientation and sliding direction

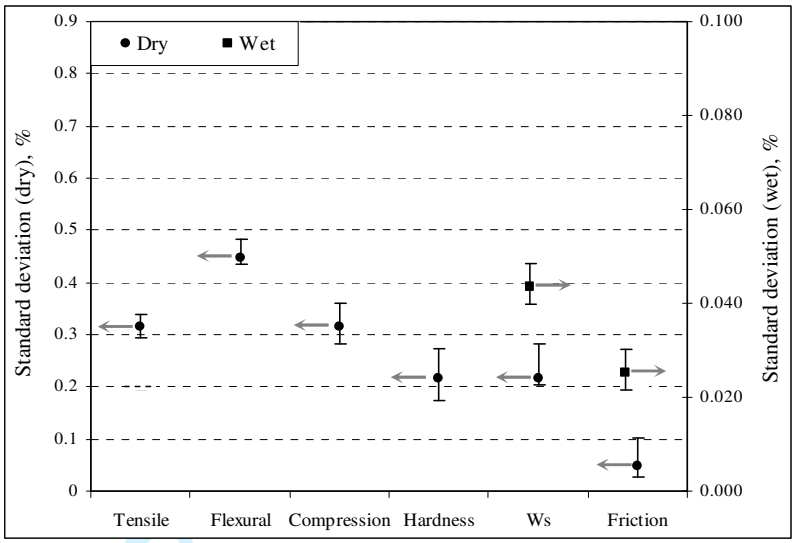

a) T-BFRP

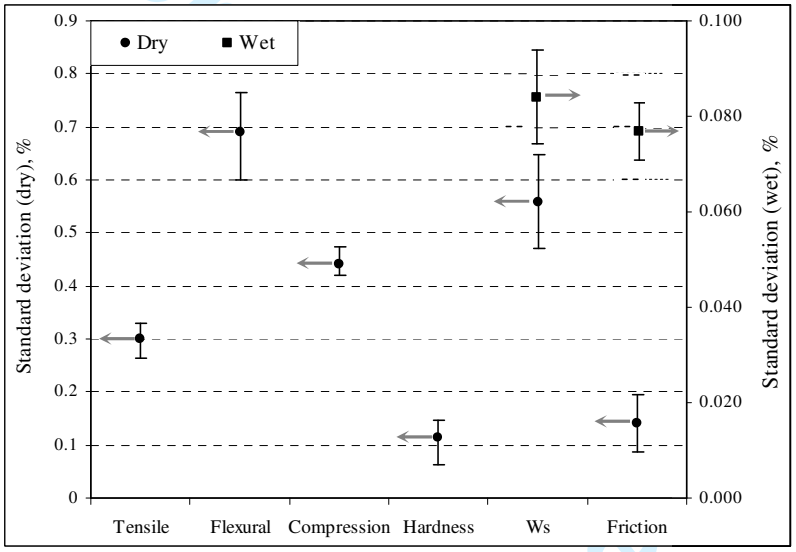

b) CSM-GFRP

Fig. 6: Corresponding standard deviation for the different types of composites

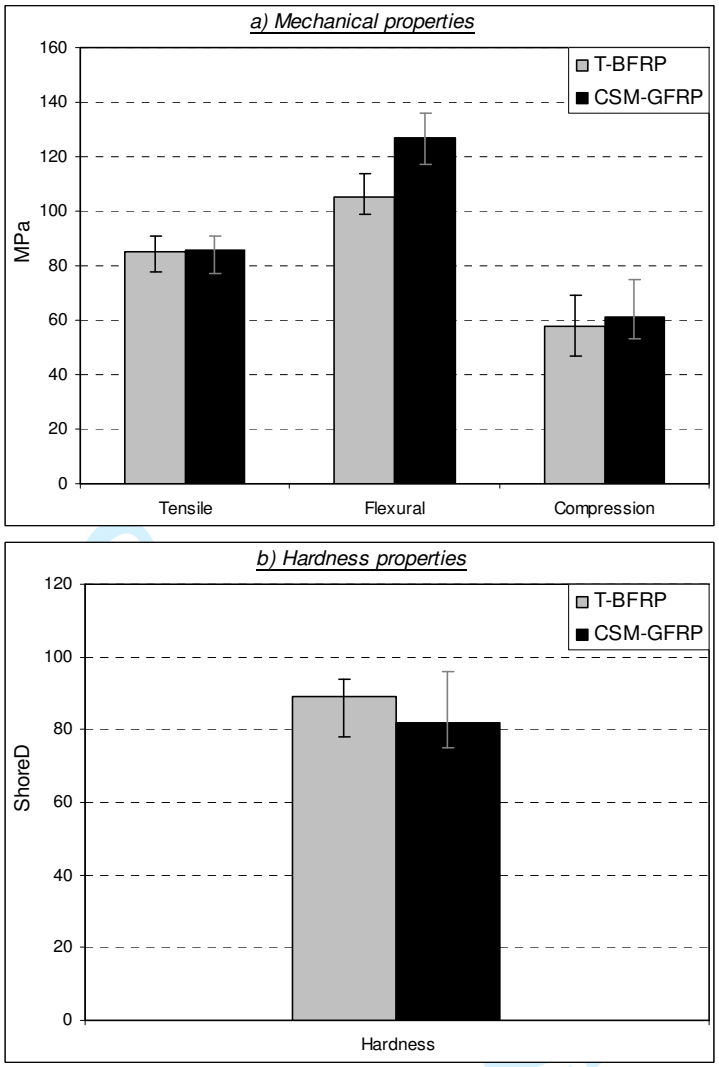

Fig. 7: Mechanical performance of T-BFRP and CSM-GFRP composites

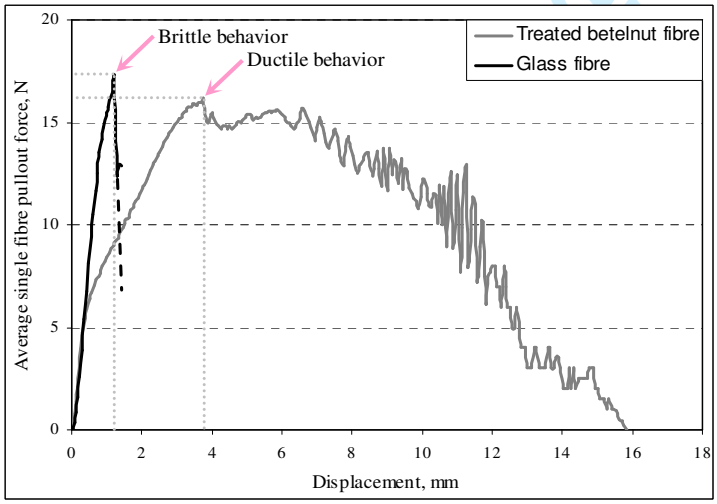

Fig. 8: SFPT for glass and treated betelnut fibre

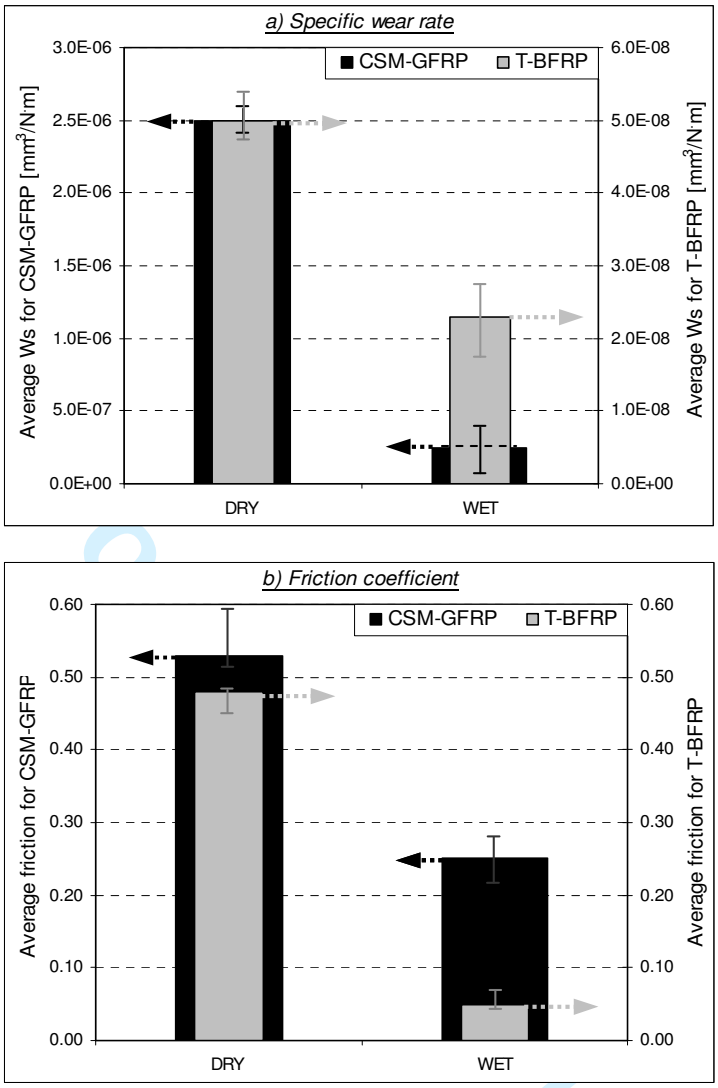

Fig. 9: Tribological performance of T-BFRP and CSM-GFRP composites

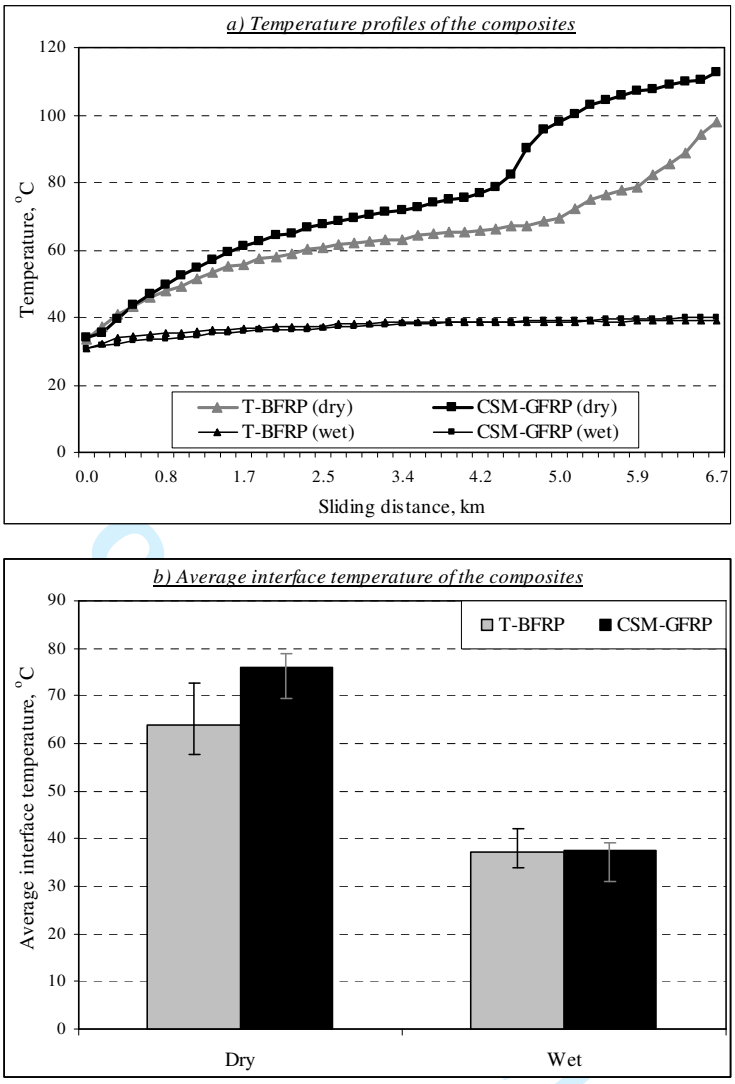

Fig. 10: Temperature performance of the T-BFRP and CSM-GFRP composites at dry and wet conditions

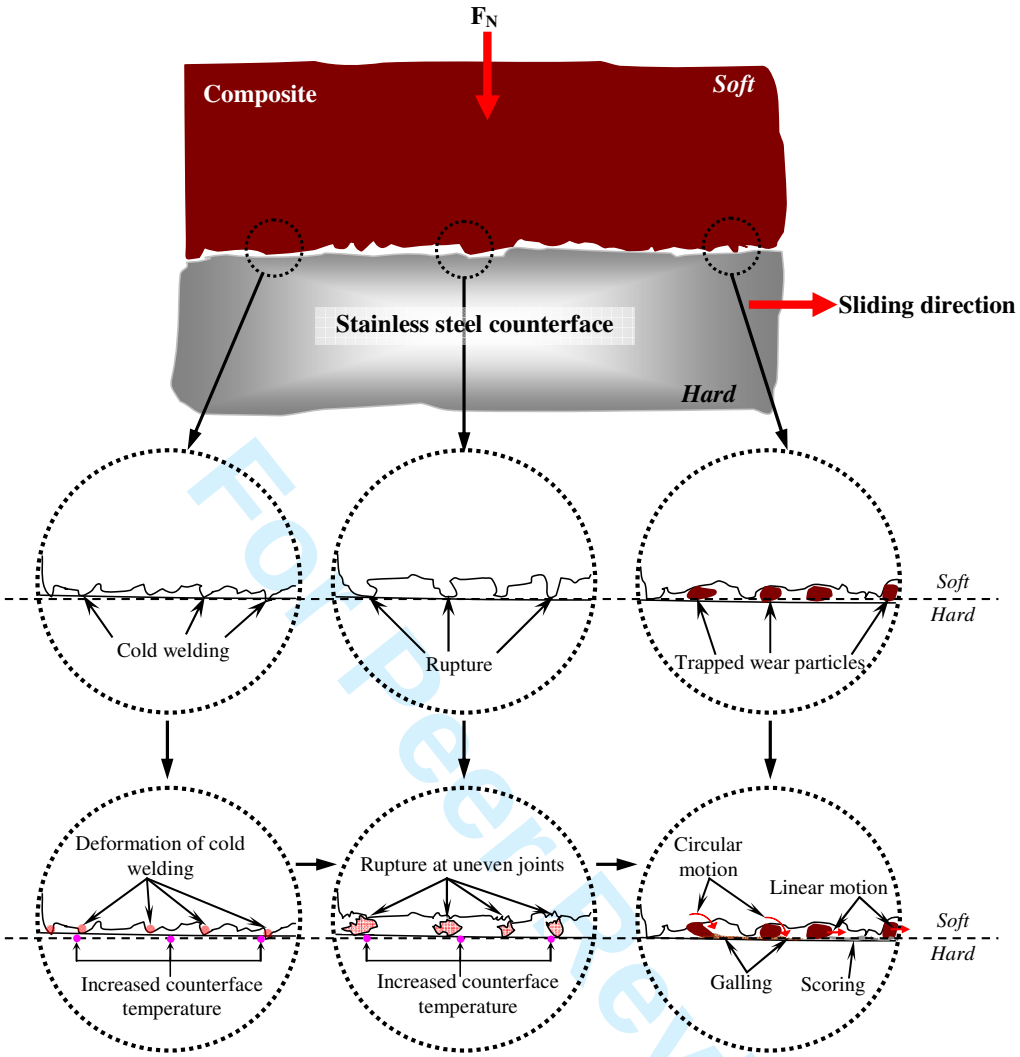

a) Sliding mechanism for adhesive dry test

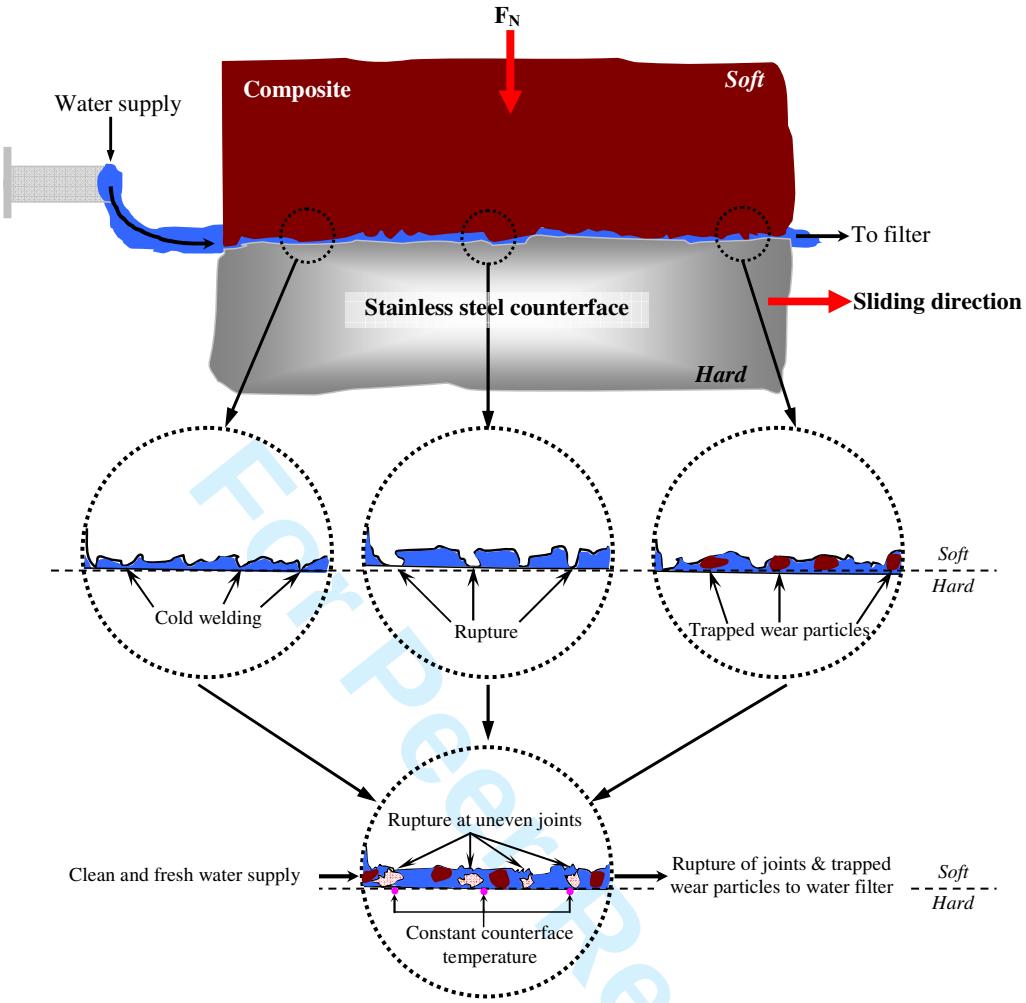

b) Sliding mechanism for adhesive wet test

Fig: 11: Adhesive sliding mechanism for dry and wet contact conditions

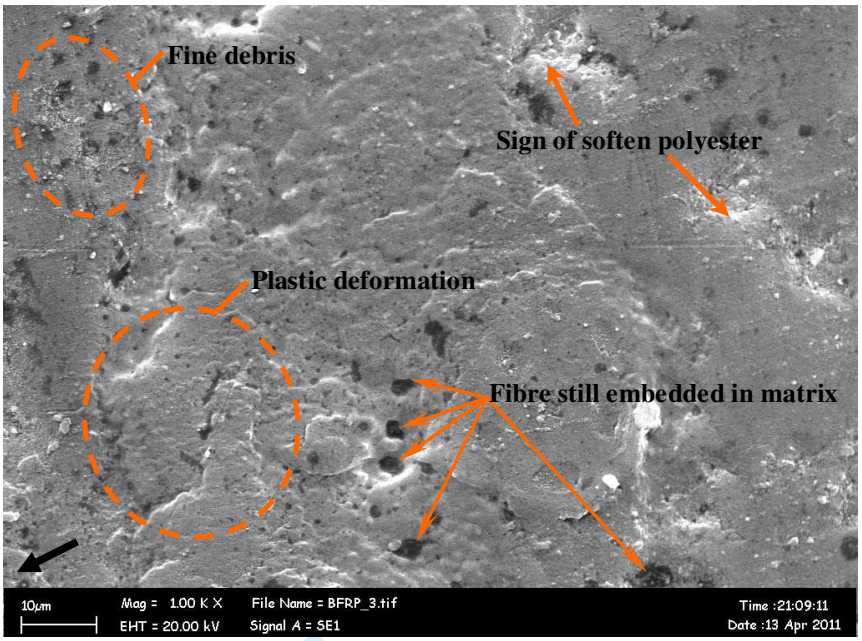

a) T-BFRP

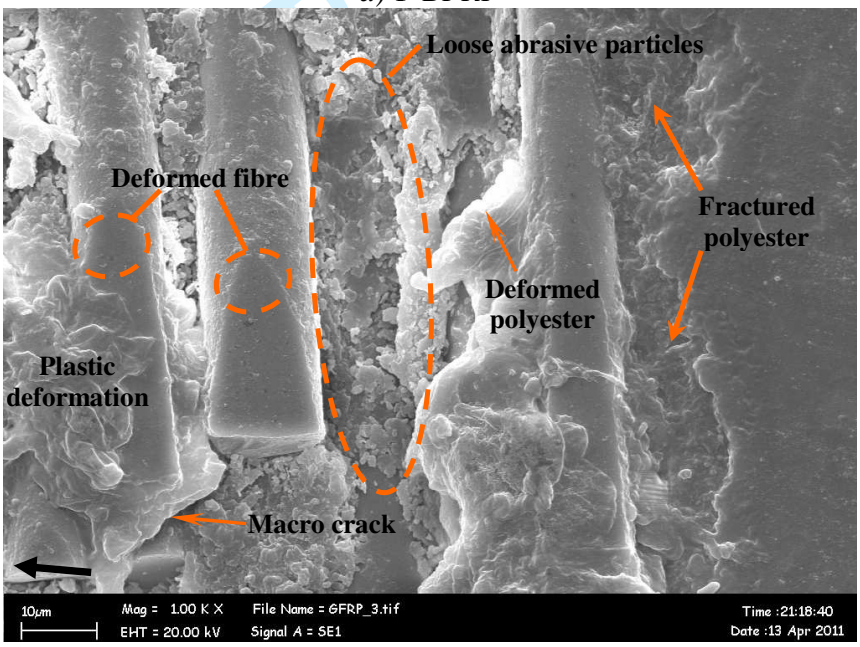

b) CSM-GFRP

Fig. 12: SEM images of the T-BFRP and CSM-GFRP composites at dry contact condition subjected to an applied load of 30 N, 6.72 km sliding distance and 2.8 m/s of counterface sliding velocity

Table 1: Average chemical composition (%) for betelnut fiber [23]

Chemical composition	Average (%)
Cellulose:	35.0 – 64.8
Lignin:	13.0 – 26.0
Pectin:	9.2 – 15.4
Nitrogen:	1.0 – 1.1
Potassium pentoxide:	0.4 – 0.5
Potassium oxide:	1.0 – 1.5

Table 2: Comparison between betelnut and CSM-glass fibers

Parameters	Betelnut fibers	CSM-glass fibers
Density:	0.019-0.021 g/cm^3	0.045-0.064 g/cm^3 [18]
Cost:	Highly abundant	\$1.50-\$2.00/kg [6, 30]
Renewability:	Yes	No
Recyclability:	Yes	No
Energy consumption:	Low	High
Distribution:	Wide	Wide
CO_2 neutral:	Yes	No
Abrasion to machines:	Low – fibres are soft	Yes – fibres are hard
Health risk:	No	Yes
Disposal:	Biodegradable	Non-biodegradable

Table 3: Basic properties of betelnut and CSM glass fibers

Parameters	Betelnut fibers	CSM glass fibers
Thickness of the mat:	150 – 180 µm	160 – 200 µm
Length of individual fibers in mat:	20 – 50 mm	10 – 60 mm
Range of the fiber diameters in mat:	100 µm – 200 µm	50 µm – 100 µm
Density of fiber mat:	200 ± 10 g/m^2	450 g/m^2
Average distance of fibers in the mat:	83 ± 5 µm	60 ± 5 µm
Size of the mat:	100 mm x 100 mm	
Orientation of fibres in the mat:	Randomly distributed	
Fibre loading:	48vol.%	

Table 4: Specifications of the resin and hardener[32]

Resin:	Unsaturated polyester Butanox M-60
Color:	Colorless
Density:	1370 kg/m^3 (20^{o}C)
Hardness:	84 ± 2 ShoreD
Hardener:	**Methyl Ethyl Ketone Peroxide (MEKP)**
Color:	Colorless
Density:	1170 kg/m^3 (20^{o}C)
Specific gravity:	1.05 – 1.06 (20^{o}C)
Percentage used:	1.25% (wt)